Instability and Evolution of Nonlinearly Interacting Capillary Gravity Waves Over Finite Depth

Shibam Manna, Tanmoy Pal and Asoke Kumar Dhar

Abstract

Two-dimensional coupled nonlinear Schrödinger equations have been established for nonlinearly interacting capillary gravity waves over finite water depths. These evolution equations are then used to examine the instability properties of two Stokes wave trains for unidirectional and bidirectional perturbations. The drawn figures exhibit the instability growth rate for distinct water depth values and for various angles of the interaction of two-wave trains. These figures demonstrate that rogue waves can be generated due to modulational instability in obliquely propagating waves over a finite water depth. Furthermore, it is found that the instability growth rate over a limited depth of water for obliquely propagating waves is much elevated than that for an infinite depth of water, and it enhances as the water depth decreases. We have also examined the effect of capillarity on Benjamin–Feir's instability.

Keywords

Coupled nonlinear Schrödinger equation · Capillary gravity waves · Modulational instability

1 Introduction

There has been considerable interest in studying the occurrence of rogue waves. The concept of rogue waves, introduced by Drapper (1966), can be generated due to both nonlinear and statistical effects and may occur in infinite and finite water depths (Shukla et al., 2006). Based on two-coupled third-order nonlinear Schrödinger equations (NLSE), Roskes (1976) has studied the instability analysis for surface gravity wave in the presence of second wave in deep water. Dhar and Das (1991) have extended that result starting from the fourth-order nonlinear evolution equation. A further extension of that result to include capillarity has been performed by Dhar and Das (1993). Onorato et al. (2006) have established two-coupled nonlinear Schrödinger equations in the case of two nonlinearly interacting wave systems in infinite water depths and traveling in two different directions. Then, they have studied the instability analysis in the case of unidirectional perturbation. That analysis has been extended by Shukla et al. (2006) to obtain the instability growth rate for bidirectional perturbations. Laine Pearson (2010) has discussed the interaction of two weekly nonlinear wave trains for distinct carrier frequencies and traveling in two separate directions, similar to obliquely interacting waves. He has demonstrated that the instability growth rate for more general two-wave trains can be larger than for short crested waves. Kundu et al. (2013) have also established nonlinear evolutions for two gravity wave packets for a finite depth of water and interacting obliquely on the surface of the water. The creation of rogue waves due to modulational instability of two obliquely propagating wave trains has been discussed by Didenkulova (2011), Gramstad and Trulsen (2010), Hjelmervik and Trulsen (2009), Onorato et al. (2010, 2011). All these investigations that the authors above have performed are for gravity waves. Recently, Manna and Dhar have made a paper on two obliquely acting capillary gravity waves in the water of infinite depth (Manna & Dhar, 2021a), and they have obtained the solutions of coupled third-order NLSE in the (x-t) space (Manna & Dhar, 2021b) for the same problem. The present paper deals with three-coupled third-order nonlinear Schrödinger equations for obliquely interacting capillary gravity waves over finite

S. Manna (✉) · T. Pal · A. K. Dhar
Indian Institute of Engineering Science and Technology, Shibpur, India
e-mail: mannashibam31@gmail.com

S. Manna
Department of Engineering and Technological Studies, University of Kalyani, Kalyani, West Bengal 741235, India

water depth. In this case, two capillary gravity wave trains travel obliquely and form equal angles with the direction of propagation, which is considered as x axis. Therefore, this paper is an extension of the work made by Kundu et al. (2013) to include capillarity.

2   Fundamental Equations

We consider the free surface in the undisturbed situation as the $z = 0$ plane, and z axis is taken vertically upwards. We take two capillary gravity wave packets of wave numbers k_1, k_2, respectively, which is traveling in the xy plane. Next, we take $z = \eta(x, y, t)$ as the equation of the free surface at time t in the perturbed state. The perturbed velocity potential ϕ satisfies the three-dimensional Laplace equation

$$\nabla^2 \phi = 0, \text{in} -d < z < \eta \tag{1}$$

The boundary conditions for the wave motion are given by

$$\phi_z - \eta_t = \phi_x \eta_x + \phi_y \eta_y, \text{at } z = \eta \tag{2}$$

$$\phi_t + g\eta = -\frac{1}{2}(\nabla\phi)^2 + \frac{T\{\eta_{xx}(1 + \eta_y^2) + \eta_{yy}(1 + \eta_x^2) - 2\eta_{xy}\eta_x\eta_y\}}{(1 + \eta_x^2 + \eta_y^2)^{\frac{3}{2}}}, \text{at } z$$

$$= \eta \tag{3}$$

Also

$$\phi_z = 0, \text{at } z = -d, \tag{4}$$

where T is the ratio of the surface tension coefficient to the fluid density and g represents the acceleration due to gravity.

We look for solutions to the above equations in the form

$$Q = Q_{00} + \sum_{p=0}^{\infty}\sum_{q=0}^{\infty}\left[Q_{pq}e^{i(p\psi_1 + q\psi_2)} + c.c.\right], \quad (p = q \neq 0) \tag{5}$$

in which Q represents ϕ, η, and $c.c.$ indicates complex conjugate and $\psi_1 = k_1 x + k_2 y - \omega t$, $\psi_2 = k_1 x - k_2 y - \omega t$. In the above $\phi_{00}, \phi_{pq}, \phi_{pq}^*$ are functions of $z, x_1 = \epsilon x, y_1 = \epsilon y$ and $t_1 = \epsilon t$; $\eta_{00}, \eta_{pq}, \eta_{pq}^*$ are functions of x_1, y_1 and t_1. Here, ϵ denotes the slow ordering parameter. The linear dispersion relation is given by

$$\omega^2 - gk\mu(1 + s) = 0, \tag{6}$$

where $\mu = \tanh kd, k^2 = k_1^2 + k_2^2$ and $s = \frac{Tk^2}{g}$.

The group velocity of each of the two-wave packets is as follows

$$c_g = \frac{c_p}{2\mu(1 + s)}\{\mu(1 + 3s) + kd(1 - \mu^2)(1 + s)\},$$

where $c_p = \omega/k$ represents the phase velocity.

3   Derivation of Evolution Equations

Following Kundu et al. (2013) and making dimensionless the variables by the relations given by

$$(x_1, y_1, \eta_{10}, \eta_{01}, d) = (kx_1, ky_1, k\eta_{10}, k\eta_{01}, kd).$$

$$t_1 = \omega t_1, (k_1, k_2) = \left(\frac{k_1}{k}, \frac{k_2}{k}\right), \tilde{\phi} = \phi_{00}^{(1)}/\frac{\omega}{k^2}, \tag{7}$$

and finally, using the transformation

$$\xi = x_1 - \overline{c_g}t_1, \eta = y_1, \tau = \epsilon t_1, \tag{8}$$

we obtain the third-order nonlinear evolution equations consisting of three-coupled equations for crossing sea states

$$2i\frac{\partial\eta_{10}}{\partial\tau} + i\delta_1 k_2\frac{\partial\eta_{10}}{\partial\eta} + \delta_2\left(k_1\frac{\partial}{\partial\xi} + k_2\frac{\partial}{\partial\eta}\right)^2\eta_{10}$$

$$+ \delta_3\left(k_2\frac{\partial}{\partial\xi} - k_1\frac{\partial}{\partial\eta}\right)^2\eta_{10} \tag{9}$$

$$= \left(\mu_1|\eta_{10}|^2 + \mu_2|\eta_{01}|^2\right)\eta_{10} + \eta_{10}P_1\tilde{\phi}$$

$$2i\frac{\partial\eta_{01}}{\partial\tau} - i\delta_1 k_2\frac{\partial\eta_{01}}{\partial\eta} + \delta_2\left(k_1\frac{\partial}{\partial\xi} - k_2\frac{\partial}{\partial\eta}\right)^2\eta_{01}$$

$$+ \delta_3\left(k_2\frac{\partial}{\partial\xi} + k_1\frac{\partial}{\partial\eta}\right)^2\eta_{01} \tag{10}$$

$$= \left(\mu_1|\eta_{01}|^2 + \mu_2|\eta_{10}|^2\right)\eta_{01} + \eta_{01}P_2\tilde{\phi}$$

and

$$\left(\gamma_1\frac{\partial^2}{\partial\xi^2} + \gamma_2\frac{\partial^2}{\partial\eta^2}\right)\tilde{\phi} = P_1|\eta_{10}|^2 + P_2|\eta_{01}|^2, \tag{11}$$

in which the forms of P_1, P_2 are

$$P_1 \equiv \{2 + (1 - \mu^2)\overline{c_g}\}k_1\frac{\partial}{\partial\xi} + 2k_2\frac{\partial}{\partial\eta},$$

$$P_2 \equiv \{2 + (1 - \mu^2)\overline{c_g}\}k_1\frac{\partial}{\partial\xi} - 2k_2\frac{\partial}{\partial\eta}, \tag{12}$$

$$\gamma_1 = k_1^2\mu^2\overline{c_g}^2 - \frac{\mu d}{1 + s}, \gamma_2 = -\frac{\mu d}{1 + s},$$

where $\overline{c_g} = c_g/c_p$ and the coefficients of Eqs. (9) and (10) are available in the Appendix. To render the results acceptable, comparing them with other results is useful. For example, in the absence of surface tension, the Eqs. (9) to (11) reduce to the corresponding equations of S. Kundu et al. (2013). Further, for $s = 0$ and in the limit $d \to \infty$, the coefficients appearing on the said equations reduce to those of Onorato et al. (2006) and Shukla et al. (2006).

4   Stability Analysis and Results

The solutions of the uniform wave trains are given by

$$\eta_{10} = \alpha_0 e^{-i\tau \Delta \omega_1}$$
$$\eta_{01} = \beta_0 e^{-i\tau \Delta \omega_2}, \overline{\phi} = \overline{\phi}_0 \quad (13)$$

in which $\alpha_0, \beta_0, \overline{\phi}_0$ are real constants, and the frequency shifts due to nonlinearity are

$$2\Delta\omega_1 = \mu_1 \alpha_0^2 + \mu_2 \beta_0^2, 2\Delta\omega_2 = \mu_1 \beta_0^2 + \mu_2 \alpha_0^2 \quad (14)$$

Next, we consider the small perturbations $\alpha_p, \beta_p, \phi_p$ given by

$$\eta_{10} = \alpha_0 (1 + \alpha_p) e^{-i\tau \Delta \omega_1}, \eta_{01}$$
$$= \beta_0 (1 + \beta_p) e^{-i\tau \Delta \omega_2}, \overline{\phi} = \overline{\phi}_0 (1 + \phi_p). \quad (15)$$

Inserting (15) in three Eqs. (9), (10), (11), linearizing and taking Fourier transform defined by

$$\overline{g}(\lambda, \sigma) = \frac{1}{2\pi} \int\limits_{-\infty}^{+\infty}\!\!\int g(\xi, \eta) e^{-i(\lambda\xi + \sigma\eta)} d\xi d\eta , \quad (16)$$

we obtain the nonlinear dispersion relation given by

$$\left[(2\overline{\Omega} - \delta_1 k_2 \sigma)^2 - A_+ \{A_+ + 2(\mu_1 + CB_+^2)\alpha_0^2\} \right]$$
$$\left[(2\overline{\Omega} + \delta_1 k_2 \sigma)^2 - A_- \{A_- + 2(\mu_1 + CB_-^2)\beta_0^2\} \right] \quad (17)$$
$$= 4A_+ A_- (\mu_2 + CB_+ B_-)^2 \alpha_0^2 \beta_0^2,$$

where $\overline{\Omega}$ represents the perturbed frequency and $A_\pm, B_\pm, C$ are given by

$$A_\pm = \delta_2(k_1\lambda \pm k_2\sigma)^2 + \delta_3(k_2\lambda \mp k_1\sigma)^2,$$

$$B_\pm = \{2 + (1 - \mu^2)\overline{c_g}\}k_1\lambda \pm 2k_2\sigma, C = \frac{1}{(\gamma_1\lambda^2 + \gamma_2\sigma^2)}. \quad (18)$$

In Figs. 1 and 2, we have plotted a contour plot of the instability growth rate $G_r = \Omega_i$. From the figures, we have observed that the instability growth rate increases due to the effect of capillarity. Further, in Fig. 1, we have seen that the instability growth rate is slightly elevated as compared to Fig. 2. Also, in both subfigures of Fig. 3 and the left subfigure of Fig. 4, it is seen that the instability growth

Fig. 1 Contour plot of instability growth rate $G_r = \Omega_i$ in (λ, σ) plane for $\alpha_0 = \beta_0 = 0.1, h = 2, s = 0$ (left), $s = 0.035$ (right)
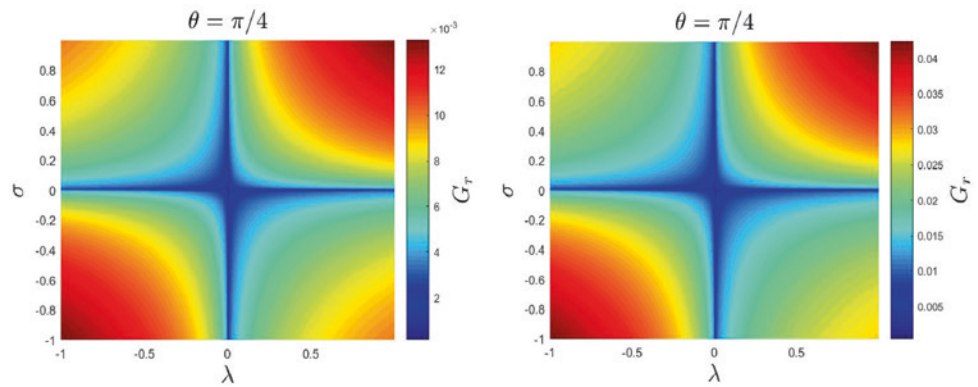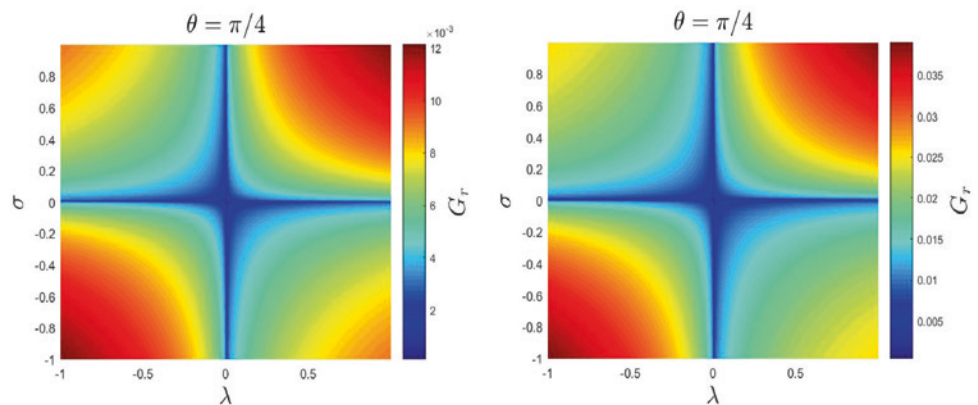

Fig. 2 Contour plot of instability growth rate $G_r = \Omega_i$ in (λ, σ) plane for $\alpha_0 = 0.12, \beta_0 = 0.07, h = 2, s = 0$ (left), $s = 0.035$ (right)
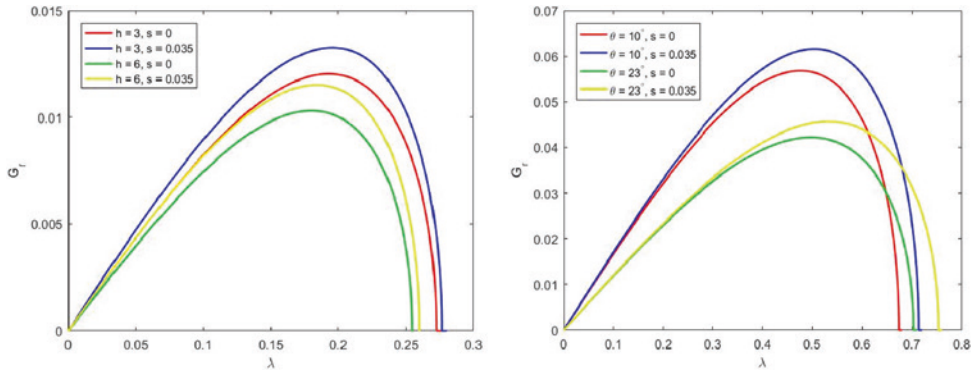
Fig. 3 Instability growth rate $G_r = \Omega_i$ for $\alpha_0 = \beta_0 = 0.1, \theta = 75°, h = 3, 6, s = 0, 0.035$ (left); for $\alpha_0 = \beta_0 = 0.1, h = 2.5, \theta = 10°, 23°, s = 0, 0.035$ (right)
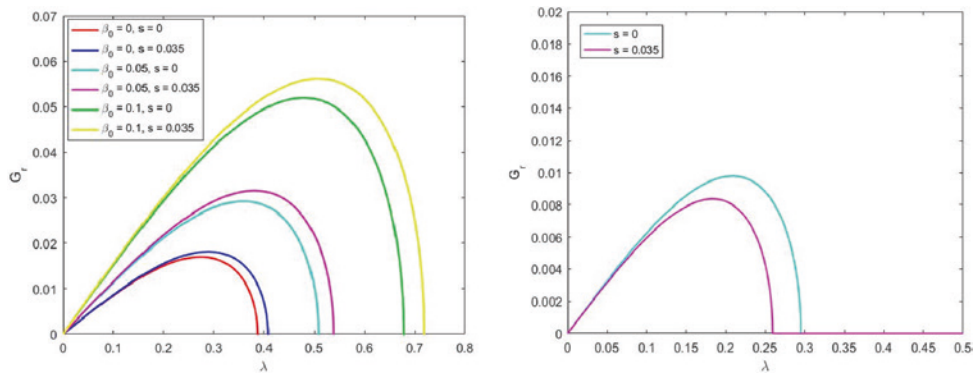

Fig. 4 Instability growth rate $G_r = \Omega_i$ for $\alpha_0 = 0.1, h = 2.5, \theta = 15°, \beta_0 = 0, 0.05, 0.1, s = 0, 0.035$ (left); for $\alpha_0 = \beta_0 = 0.1, h \to \infty, \theta = 75°, s = 0, 0.035$ (right)

rate increases due to the capillarity effect. Furthermore, from these subfigures, we infer that G_r increases with the increment of water depth h as well as the wave steepness β_0 of the second wave, whereas G_r decreases as the angle θ between the two waves increases. Finally, from the right subfigure of Fig. 4, in the case of infinite depth fluid, the reverse effect of capillarity is noticed, and the instability growth rate is reduced as compared to finite depth fluid.

5   Conclusion

We have established two-coupled third-order NLSE for obliquely propagating capillary gravity waves over finite depth, which are valid for any water depth values apart from shallow water depth. Based on these NLSE, stability analysis is then made for two Stokes wave systems. Figures that have been drawn demonstrate the instability growth rate for different water depth values and various angles of the interaction of two-wave trains. It is observed from the graphs that the growth rate of instability over a finite depth

of water for obliquely interacting wave trains is much elevated than the case of modulation in deep water, and it increases as the water depth decreases. Further, the instability growth rate for obliquely propagating wave trains is again much higher than the case of modulation for single wave trains. We have also investigated the effect of capillarity on modulational instability.

Appendix

$$\delta_1 = \frac{1 + 3s}{1 + s} + \frac{h(1 - \mu^2)}{\mu},$$

$$\delta_2 = \frac{1}{4}\left[\frac{2h(1 + 3s)(1 - \mu^2)}{(1 + s)\mu} - \frac{1}{1 + s} - \frac{(1 - \mu^2)(1 + 3\mu^2)h^2}{\mu}\right],$$

$$\delta_3 = \frac{\delta_1}{2},$$

$$\mu_1 = \left(\frac{9 - 12\mu^2 + 13\mu^4 - 2\mu^6}{2\mu^4}\right)\left(\frac{1 + 3s}{1 + s}\right),$$

$$\mu_2 = \frac{\left\{4\left(2k_1^2 - k_2^2\right)\mu^2 - \left(\mu^2 - 1\right)^2 - \left(k_1^2 - k_2^2 - \mu^2\right)^2\right\}(1 + 3s)}{(1 + s)\sigma^2}$$

$$- \frac{k_1(\mu \tanh 2k_1 h - 2k)\left(k_1^2 - k_2^2 - 3\mu^2\right)(1 + 2s)}{(1 + s)\mu^2}$$

$$- \frac{k_1\left\{4k_1\mu + \tanh 2k_1 h\left(k_1^2 - k_2^2 - 3\mu^2\right)\right\}\left\{k\mu \tanh 2k_1 h - 3k_1^2 + k_2^2 + \mu^2\right\}}{\left\{2\mu - \frac{k_1\left(1 + 4sk^2\right)}{1 + s}\tanh 2k_1 h\right\}\sigma^2}.$$

References

Dhar, A. K., & Das, K. P. (1991). Fourth-order nonlinear evolution equation for two Stokes wave trains in deep water. *Physics of Fluids A, 3*(12), 3021–3026.

Dhar, A. K., & Das, K. P. (1993). Effect of capillarity on fourth-order nonlinear evolution equations for two Stokes wave trains in deep water. *Journal of the Indian Institute of Science, 73*, 579.

Didenkulova, I. (2011). Shapes of freak waves in the coastal zone of Baltic Sea (Tallinn Bay). *Boreal Environment Research*, *16*(Suppl. A), 138–148.

Draper, L. (1966). Freak ocean waves. *Weather, 21*(1), 2–4.

Gramstad, O., & Trulsen, K. (2010). Can swell increase the number of freak waves in a wind-sea? *Journal of Fluid Mechanics, 650*, 57–79.

Hjelmervik, K. B., & Trulsen, K. (2009). Freak wave statistics on collinear currents. *Journal of Fluid Mechanics, 637*, 267–284.

Kundu, S., Debsarma, S., & Das, K. P. (2013). Modulational instability in crossing sea states over finite depth water. *Physics of Fluids, 25*, 066605.

Laine-Pearson, F. E. (2010). Instability growth rates of crossing sea states. ***Physical Review E, 81***, 036316-1-7.

Manna, S., & Dhar, A. K. (2021a). Modulational instability of obliquely interacting capillary-gravity waves over infinite depth. *Archives of Mechanics, 73*(5–6), 583–598.

Manna, S., & Dhar, A. K. (2021b). Analytical solutions of coupled nonlinear Schrodinger equations for two nonlinearly interacting stokes wave trains over infinite depth. *Advances in Mathematics: Scientific Journal, 10*, 1137–1144.

Onorato, M., Osborne, A. R., & Serio, M. (2006). Modulational instabilities in crossing seas: A possible mechanism for the formation of freak wave. *Physical Review Letters*, *96*, 014503-1-4.

Onorato, M., Proment, D., & Toffoli, A. (2010). Freak waves in crossing seas. *The European Physical Journal Special Topics, 185*, 45–55.

Onorato, M., Promett, D., & Toffoli, A. (2011). Triggering rogue waves in opposing currents. *Physical Review Letters*, *107*, 184502-1-5.

Roskes, G. J. (1976). Nonlinear multiphase deep-water wavetrains. *19*, 1253–54.

Shukla, P. K., Kourakis, I., Eliasson, B., Marklund, M., & Stefano, L. (2006). Instability and evolution of nonlinearly interacting water wave. *Physical Review Letters*, *97*, 094501-1-4.